THE JOURNAL OF BIOLOGICAL CHEMISTRY VOL. 284, NO. 8, pp. 5097–5106, February 20, 2009

Ablation of Ventricular Myosin Regulatory Light Chain Phosphorylation in Mice Causes Cardiac Dysfunction *in Situ* and Affects Neighboring Myofilament Protein Phosphorylation*

Received for publication, September 24, 2008, and in revised form, November 19, 2008 Published, JBC Papers in Press, December 23, 2008, DOI 10.1074/jbc.M807414200

Sarah B. Scruggs[‡], Aaron C. Hinken[‡], Ariyaporn Thawornkaiwong[‡], Jeffrey Robbins[§], Lori A. Walker[¶], Pieter P. de Tombe[‡], David L. Geenen[‡], Peter M. Buttrick[¶], and R. John Solaro[‡1]

From the [‡]Department of Physiology and Biophysics and Center for Cardiovascular Research, [‡]University of Illinois at Chicago, Chicago, Illinois 60612, the [§]Department of Molecular Cardiovascular Biology, Cincinnati Children's Hospital, Cincinnati, Ohio 45229, and the [¶]Division of Cardiology, University of Colorado at Denver, Aurora, Colorado 80045

There is little direct evidence on the role of myosin regulatory light chain phosphorylation in ejecting hearts. In studies reported here we determined the effects of regulatory light chain (RLC) phosphorylation on *in situ* cardiac systolic mechanics and *in vitro* myofibrillar mechanics. We compared data obtained from control nontransgenic mice (NTG) with a transgenic mouse model expressing a cardiac specific nonphosphorylatable RLC (TG-RLC(P−). We also determined whether the depression in RLC phosphorylation affected phosphorylation of other sarcomeric proteins. TG-RLC(P−) demonstrated decreases in base-line load-independent measures of contractility and power and an increase in ejection duration together with a depression in phosphorylation of myosin-binding protein-C (MyBP-C) and troponin I (TnI). Although TG-RLC(P−) displayed a significantly reduced response to β_1-adrenergic stimulation, MyBP-C and TnI were phosphorylated to a similar level in TG-RLC(P−) and NTG, suggesting cAMP-dependent protein kinase signaling to these proteins was not disrupted. A major finding was that NTG controls were significantly phosphorylated at RLC serine 15 following β_1-adrenergic stimulation, a mechanism prevented in TG-RLC(P−), thus providing a biochemical difference in β_1-adrenergic responsiveness at the level of the sarcomere. Our measurements of Ca^{2+} tension and Ca^{2+}-ATPase rate relations in detergent-extracted fiber bundles from LV trabeculae demonstrated a relative decrease in maximum Ca^{2+}-activated tension and tension cost in TG-RLC(P−) fibers, with no change in Ca^{2+} sensitivity. Our data indicate that RLC phosphorylation is critical for normal ejection and response to β_1-adrenergic stimulation. Our data also indicate that the lack of RLC phosphorylation promotes compensatory changes in MyBP-C and TnI phosphorylation, which when normalized do not restore function.

Phosphorylation of sarcomeric proteins tunes the intensity and dynamics of cardiac contraction and relaxation independent of membrane Ca^{2+} fluxes to meet physiologic demands (1, 2). We focus here on ventricular myosin regulatory light chain, which is phosphorylated *in vivo* (3–5) but whose functional role in control of cardiac dynamics has remained unclear. The identification of RLC[2] mutations linked to familial hypertrophic cardiomyopathy (6) underscores the importance of understanding its action as a regulator of contraction. Functionally, *in vitro* cardiac RLC phosphorylation by MLCK produces a sensitizing shift in the force-Ca^{2+} relation in skinned fibers (7–11). Moreover, studies show that RLC phosphorylation manifests as a gradient across the wall of the heart, which may be important for both normalizing wall stress and for generation of torsion about the long axis of the ejecting heart (12–14). Yet there remains a lack of understanding of the *in situ* functional effects of RLC phosphorylation and whether phosphorylation of RLC influences other sarcomeric sites as substrates for kinases and phosphatases.

Understanding the precise mechanisms by which phosphorylation of RLC affects function of ejecting ventricles is particularly important, because mechanisms downstream of Ca^{2+} fluxes at the level of the sarcomere appear to dominate ejection and to sustain ventricular elastance (15). Myosin motors are important in this, and RLC is well positioned at the S1-S2 junction to modulate myosin heavy chain directly by fine-tuning lever arm motion and indirectly by interacting with the essential light chain, the thick filament backbone, and MyBP-C (16, 17). Accordingly, the hypothesis underlying this study was that ablation of N-terminal RLC phosphorylation would elicit a depression in ventricular ejection and compensatory changes in phosphorylation of sarcomeric proteins neighboring RLC.

To understand the role of RLC phosphorylation in the ejection phase of the cardiac cycle, we determined *in situ* pressure-volume functions in ejecting, auxotonically loaded ventricles expressing either wild type RLC (NTG) or a nonphosphorylat-

* This work was supported, in whole or in part, by National Institutes of Health Grants PO1 HL62426 (to R. J. S., P. P. D., and P. M. B.), RO1 HL22231 (to R. J. S.), T32 HL07962 (to S. B. S. and A. C. H.), and F32 HL086023 (to A. C. H.). This work was also supported by American Heart Association Grant 0710031Z (to S. B. S.) and funds from the Temple Hoyne Buell Foundation. The costs of publication of this article were defrayed in part by the payment of page charges. This article must therefore be hereby marked "*advertisement*" in accordance with 18 U.S.C. Section 1734 solely to indicate this fact.

[1] To whom correspondence should be addressed: 835 South Wolcott Ave., M/C 901, Chicago, IL 60612. Tel.: 312-996-7620; Fax: 312-996-1414; E-mail: solarorj@uic.edu.

[2] The abbreviations used are: RLC, muscle thick filament protein myosin regulatory light chain; LV, cardiac left-ventricle; MyBP-C, muscle thick filament protein myosin-binding protein-C; TnI, inhibitory subunit of cardiac troponin; PKA, cyclic AMP-dependent protein kinase; MLCK, myosin light chain kinase; ESPVR, the slope of the end systolic pressure-volume relationship; NTG, nontransgenic mice; CHAPS, 3-[(3-cholamidopropyl)dimethylammonio]-1-propanesulfonic acid.

able RLC (TG-RLC(P−)) (10). Our experiments provide novel data demonstrating the importance of RLC phosphorylation in systolic pump function and provide new insights into how a lack of phosphorylation of RLC induces a redistribution of charge among myofilament proteins. Furthermore, our data demonstrate an enigmatic blunting of TG-RLC(P−) functional response to β_1-adrenergic simulation despite a normal TnI and MyBP-C phosphorylation profile. RLC serine 15 phosphorylation increased significantly in NTG controls but was not permitted in TG-RLC(P−) (RLC S14/15/19/A), suggesting that a change in RLC phosphorylation following β_1-adrenergic simulation may be critical for eliciting a normal response.

EXPERIMENTAL PROCEDURES

Animals—The experiments were carried out according to guidelines instituted by the Animal Care and Use Committee at the University of Illinois at Chicago (ACC number 05-240). TG-RLC(P−) were bred from Line 21 originally described by Sanbe *et al.* (10) that expressed ~2.5-fold transgenic mRNA relative to endogenous transcript but resulted in stoichiometric replacement of endogenous RLC.

Myofilament Enrichment and Sample Preparation—Subcellular fractionation proceeded according to methods previously described (18) with modifications. The hearts were excised and immediately placed on ice in relaxed buffer: 75 mmol/liter KCl, 10 mmol/liter imidazole (pH 7.2), 2 mmol/liter $MgCl_2$, 2 mmol/liter EDTA, 1 mmol/liter NaN_3, with 1% Triton X-100, phosphatase inhibitor mixture I (Calbiochem, San Diego, CA), and protease inhibitor mixture (Sigma-Aldrich). Tissue was homogenized and centrifuged (18,000 × *g*, 10 min, 4 °C), and the supernatant was removed. The subsequent pellet following four extractions was washed, then extracted in isoelectric focusing buffer (8 mol/liter urea, 2 mol/liter thiourea, 4% CHAPS), and clarified, and the soluble fraction was frozen at −80 °C until analysis.

Narrow Range Two-dimensional PAGE for RLC Phosphorylation Quantification—The hearts were fractionated as described above, and the pellets were solubilized in isoelectric focusing buffer plus 100 mmol/liter dithiothreitol, protease inhibitor mixture (Sigma-Aldrich), and phosphatase inhibitor mixture I (Calbiochem). Protein (75 μg) was loaded on capillary tube gels (7 × 1 mm, 6.8% acrylamide, pI 4.5–5.4), focused (300 V, 16 h), and separated using SDS-PAGE. The gels were stained with ProQ Diamond (Invitrogen) followed by Sypro Ruby (Invitrogen) according to the manufacturer's protocol. The gels were imaged on an Imager FX (Bio-Rad), and the spot densities were quantified using ImageJ. The percentage of RLC phosphorylation was expressed as phospho-RLC/(unphospho-RLC + phospho-RLC) × 100%.

In Situ Pressure-Volume Analysis—Methods followed (19) with modifications. Male and female mice 13 weeks of age were sedated with etomidate (8 μg/g of body weight) administered intraperitoneally, intubated, and ventilated (100% O_2, 1.5% isoflurane). A 1.4 French pressure-volume catheter (Millar Instruments, Houston, TX) was inserted retrograde into the LV across the aortic valve, and steady-state hemodynamics were recorded using Chart5 software (ADInstruments, Colorado Springs, CO). A midline incision was made to locate the supradiaphragmatic inferior vena cava. Venous return to the heart was briefly occluded to generate a series of descending loops for deriving the slope of the end systolic pressure-volume relationship. To acutely challenge the animals, dobutamine (5 ng/g of body weight/min) was infused (1 μl/min) for 5 min intravenously via the left femoral vein. Pressure-volume traces were analyzed using PVAN 2.9 software (Millar Instruments). TG-RLC(P−) and NTG animals had similar sized ventricular cavities and wall thickness; therefore volume measurements were not corrected for parallel conductance. A series of loops was selected during steady state, and the hemodynamic parameters were averaged. For measures of contractility, loops from an inferior vena cava occlusion were selected, and algorithms inherent to PVAN 2.9 were used to calculate $E(t)$ (time-varying elastance), ESPVR, E_{max} (maximal elastance), and T_{max} (time from the onset of ejection to E_{max}). $E(t)$, was calculated from isochrones for R to R-wave time intervals using $P(t)/[V(t) - V_o]$, with V_o being the minimal volume required for the left ventricle to generate supra-atmospheric pressure (20). The isochrone of maximal steepness was deemed E_{max}. The time from the first peak of $E(t)$ trace (end of isovolumic contraction) to the maximal peak, E_{max}, was deemed T_{max}. For dobutamine studies, steady-state and occlusion data following dobutamine administration were normalized to base-line recordings from the same animal; therefore each animal served as its own control to calculate the percentage of change.

One-dimensional SDS-PAGE for Determination of Myosin Isoforms—Myofilament-enriched samples from NTG and TG-RLC(P−) mice were solubilized in 8 mol/liter urea, 2 mol/liter thiourea, 50 mmol/liter Tris (pH 6.8), 75 mmol/liter dithiothreitol, 3% SDS. 12% one-dimensional SDS-PAGE (160 × 180 mm) gels were prepared as described (21). The proteins were run at 16 mA for 4.25 h at 10 °C. The gels were fixed (50% methanol/10% acetic acid), and stained for total protein with Sypro Ruby. Fluorescence was detected using a Typhoon 9410 imager to determine the presence or absence of β-myosin heavy chain.

β_1-Adrenergic Receptor Density and Binding Assay—β_1 receptor densities and ligand binding affinities were calculated using methods previously described (22, 23) with modifications. The membranes were prepared from samples of LV homogenized in ice-cold 10 mmol/liter Tris-HCl, pH 8.0, and then incubation in 1 mol/liter KCl to dissolve the myofilament proteins. The homogenate was filtered through several layers of cheesecloth, and the filtrate was centrifuged (43,900 × *g*, 4 °C, 20 min). The pellet was resuspended in Tris buffer, homogenized, and sedimented. The final pellet was dispersed in ice-cold 50 mmol/liter HEPES, pH 8.0, and immediately used for the β_1-receptor binding assay, which was performed under equilibrium condition in various concentrations of [^{3}H]dihydroalprenolol (specific activity, 117.8 Ci/mmol; PerkinElmer Life Sciences). Nonspecific binding was analyzed in a parallel set of experiments with the addition of atenolol, a β_1 antagonist. Saturation binding was determined from the relationship between specific binding and free ligand using nonlinear least square regression analysis. Binding parameters, including the density and dissociation constant of the receptors, were determined from a linear transformation of data to the Scatchard plot of bound/free to bound form.

Minimal Cy Dye Labeling and Broad Range Two-dimensional PAGE for Global Myofilament Protein Assessment—Myofilament-enriched fractions, as described above, were labeled with fluorescent cyanine dyes (GE Healthcare) at 10 pmol/50 μg protein for 3 h at 4 °C. NTG and TG-RLC(P−) were labeled with Cy5 and Cy3, respectively, and in separate experiments labels were reversed to ensure that differences detected were biological and not due to dye affinity or sensitivity. The reactions were quenched with 10 nmol/liter lysine and 40 μg from each group was added to isoelectric focusing buffer plus 1.5% (v/v) Immobilized pH Gradient (IPG) 3-11 NL reagent (GE Healthcare), 1% (v/v) Destreak (GE Healthcare), and 65 mmol/liter dithiothreitol. Focusing was performed in accordance with Ref. 24 with modifications. Nonlinear 3-11 18 cm IPG strips (GE Healthcare) were actively rehydrated for 12 h at 50 V and 20y °C, and the proteins were focused in a Preotean isoelectric focusing cell (Bio-Rad) using a linear method (250 V for 15 min, 10000 V for 3 h, and 10000 V for 60000 V/h). Strips were laid on top of the 2% second dimension SDS-PAGE gels (21) and run for 4 h at 30 mA constant amperage with cooling (12 °C). The gels were imaged using a Typhoon 9410 (GE Healthcare), with Cy3 images using a 532-nm laser/580-nm BP 30 and Cy5 images using a 633-nm laser/670 BP30. The gels were scanned at 100-μm resolution, and the photomultiplier tube was set to obtain pixel intensity near 90,000 pixels. The images were analyzed using PDQuest v7.1.1 (Bio-Rad). Spot intensities were normalized against total image density to optimize gel to gel consistency and to correct for small variations in sample loading or system gain. The percentage of phosphorylation of MyBP-C and TnI was calculated using ratiometric analysis (the percentage of total protein represented in spot A = density of spot A/total density of protein A spots × 100%).

Western Blotting for Determination of Site-specific Changes in TnI and RLC Phosphorylation—Myofilament-enriched NTG and TG-RLC(P−) samples (10 μg) were dissolved in Laemmli buffer (25) and separated using 12% one-dimensional SDS-PAGE. The proteins were transferred to nitrocellulose membranes (Bio-Rad) using a CAPS buffer system (26) at 20 V for 90 min. The membranes were blocked with 5% nonfat milk. The following primary antibodies and dilutions were used: rabbit anti-TnI phospho-22/23 (1:500; Cell Signaling), mouse anti-TnI-C5 (1:5000; Fitzgerald Industries), rabbit anti-Ser(P)[15] (1:2000; a most generous gift from Dr. Neal Epstein at the National Institutes of Health), and mouse anti-RLC (1:1000; Alexxis Biochemical) overnight at 4 °C. The membranes were incubated with anti-mouse and anti-rabbit secondary antibodies (1:50,000) for 1 h at room temperature, incubated in ECL plus horseradish peroxidase substrate (GE Healthcare), and developed using Hyperfilm ECL (GE Healthcare).

In Vitro Force-ATPase Rate Measurements—The Ca^{2+} tension and Ca^{2+}-ATPase rate were measured in skinned fiber bundles from LV trabeculae, as previously described (27, 28).

Statistical Analysis—All data are expressed as the means ± S.E. of the mean. A *t* test was used to determine significant differences between two means of TG-RLC(P−) and NTG groups, and $p < 0.05$ was deemed significant.

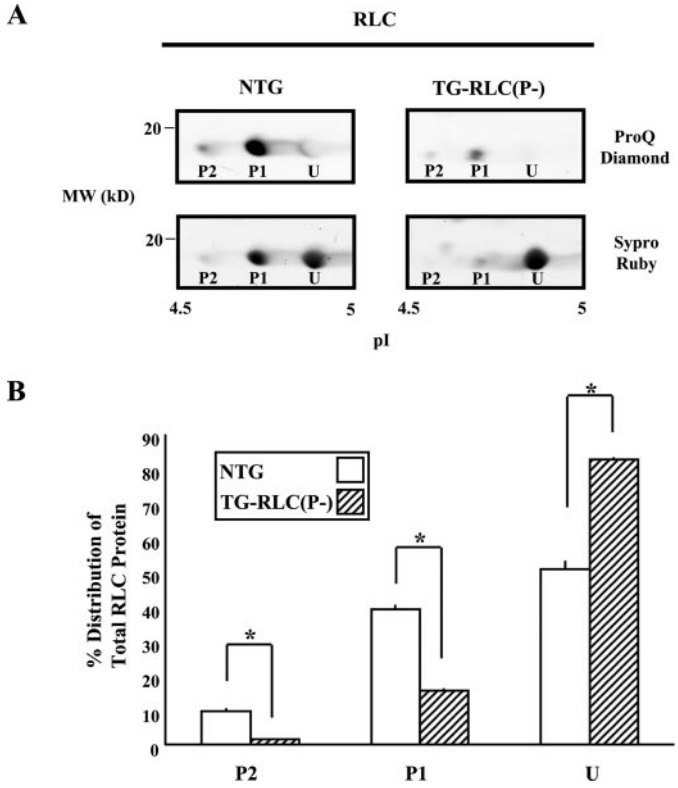

FIGURE 1. **13-week-old RLC phosphorylation in TG-RLC(P−) and NTG hearts.** *A*, representative sections of narrow-range (pI 4.5–5.0) two-dimensional PAGE gels showing two phosphorylated (*P2* and *P1*) and one unphosphorylated spot (*U*) of RLC in NTG and TG-RLC(P−). The gels were stained with the phospho-specific ProQ Diamond stain (*top panels*) and for total protein with Sypro Ruby (*bottom panels*), thus clearly illustrating the significant decrease in phosphorylation in TG-RLC(P−). *B*, percentage of RLC distribution quantified in a spot-specific manner demonstrating the significant decrease in phospho-spots P2 and P1 and increase in unphosphorylated spot U in TG-RLC(P−). The *asterisk* denotes statistical significance ($p < 0.05$; $n = 3$).

RESULTS

TG-RLC(P−) Had a 34% Deficit in RLC Phosphorylation Relative to NTG Mice—TG-RLC(P−) were used at exactly 13 weeks, a prepathologic age in which there is nearly complete RLC replacement (10). We measured the relative amount of phosphorylation in preparations isolated from TG-RLC(P−) *versus* NTG hearts with two-dimensional PAGE (Fig. 1*A*). Staining with the phospho-specific stain Pro-Q Diamond demonstrated that the two most acidic spots (P1 and P2) were phosphorylated *in vivo* with 16% (P1+P2) of RLC protein in TG-RLC(P−) phosphorylated, as compared with 50% in NTG (Fig. 1*B*).

TG-RLC(P−) Displayed Systolic Dysfunction—Fig. 2*A* shows representative base-line pressure-volume loops during an inferior vena cava occlusion. The slope of the ESPVR, a load-independent index of cardiac contractility, was significantly decreased in TG-RLC(P−) (Fig. 2*B*). End systolic volume was significantly increased in TG-RLC(P−) (Fig. 2*B*); however the decrease in stroke volume was not accompanied by an increase in end diastolic volume. Furthermore, maximal power was decreased in TG-RLC(P−) (Fig. 2*B*), presumably because of a decrease in shortening velocity in combination with a decrease in LV developed pressure (Fig. 2*A*). Moreover, stroke work was

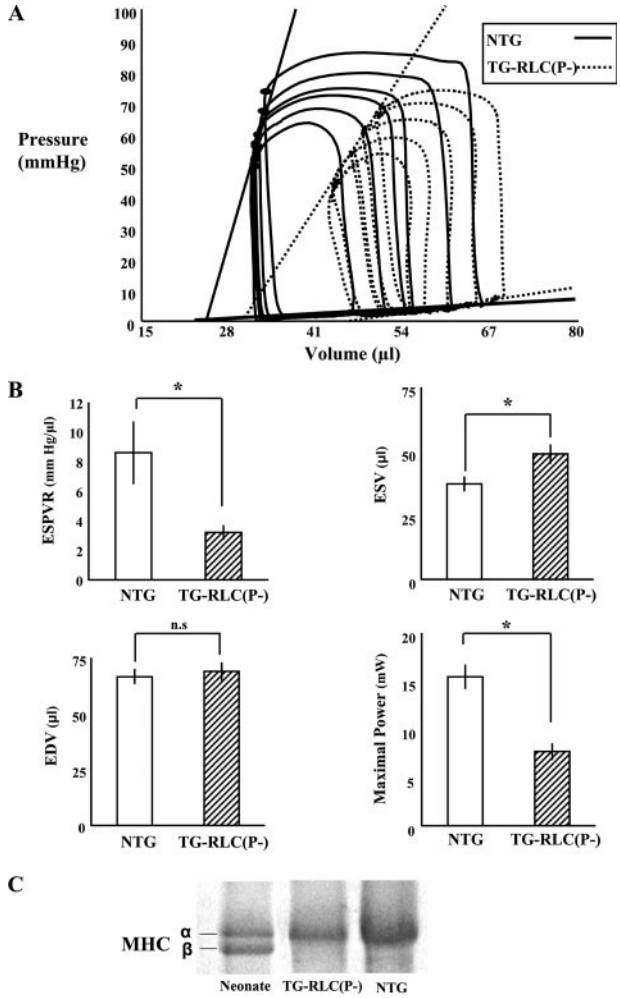

FIGURE 2. **LV Pressure-volume function and myosin heavy chain expression in TG-RLC(P−) and NTG.** *A*, base-line series of LV pressure-volume loops of NTG and TG-RLC(P−) following an inferior vena cava occlusion illustrating the significant decrease in contractility and ejection fraction in TG-RLC(P−), without a significant change in preload. *B*, select hemodynamic parameters quantifying the significant decrease in the ESPVR, the increase in end systolic volume (*ESV*), and decrease in maximal power in TG-RLC(P−), with no significant difference in end diastolic volume (*EDV*) ($n = 8–9$). The *asterisk* denotes statistical significance ($p < 0.05$). *C*, selection from a 160 × 180-mm 12% SDS-PAGE gel illustrating the separation of myosin heavy chain (*MHC*) protein in neonatal tissue (50% α/50% β isoform) and the lack of β-myosin heavy chain protein expression in the TG-RLC(P−) as in the NTG animals, indicating that the depression of contractility and maximal power are not due to an isoform shift in myosin heavy chain ($n = 3$).

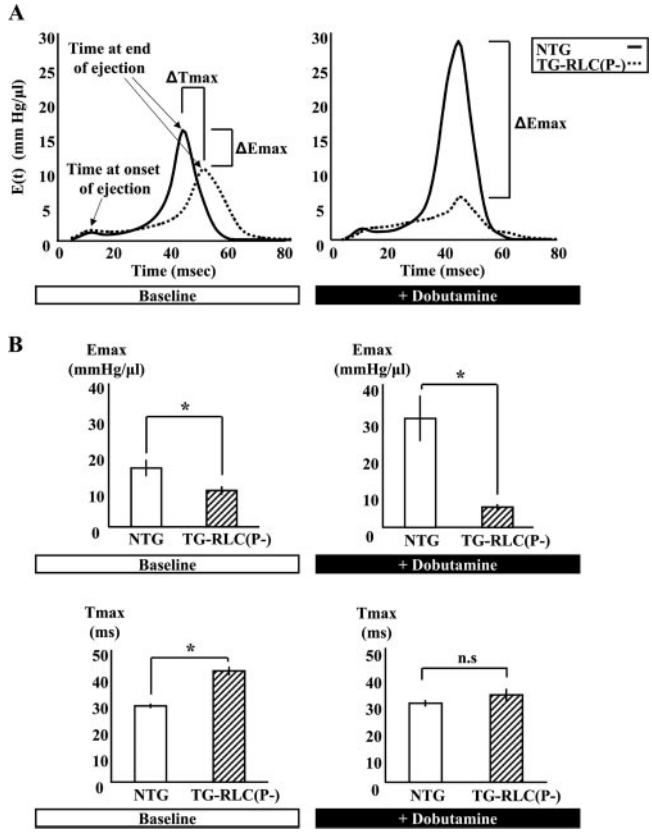

FIGURE 3. **Instantaneous pressure-volume ratio demonstrating impaired systolic elastance and kinetics in TG-RLC(P−).** *A*, representative time-varying elastance curves throughout a cardiac cycle in NTG and TG-RLC(P−) ventricles at base line (*left panel*) and following 5 min of dobutamine stimulation (*right panel*). Note the elongated ejection time (T_{max}) in TG-RLC(P−) resulting in an increased time to peak pressure at base line, which is accelerated to normal following β_1-adrenergic stimulation. Moreover, there is a dramatic decrease in maximal elastance (E_{max}) at base line in TG-RLC(P−) that persists following dobutamine stimulation, whereas that of NTG substantially increases as expected. E_{max} and T_{max}, both at base line and following β_1-adrenergic stimulation, are quantified in *B*. The *asterisk* denotes statistical significance ($p < 0.05$; $n = 5–6$).

decreased in TG-RLC(P−) with the greatest change occurring in the end systolic (upper left-hand) portion of the loop (Fig. 2*A*) in the systolic ejection phase. Importantly, these differences between TG-RLC(P−) and NTG were not due to changes in β-myosin heavy chain protein abundance (Fig. 2*C*).

Time-varying LV Chamber Elastance and Ejection Duration Were Altered in TG-RLC(P−)—To examine the kinetics of the systolic dysfunction in TG-RLC(P−) over a cardiac cycle, we determined the instantaneous pressure-volume ratio curve or time-varying elastance. $E(t)$ is a measure of LV systolic stiffening, independent of preload and afterload but exquisitely sensitive to changes in inotropic state (29). Base-line $E(t)$ curves for TG-RLC(P−) (Fig. 3*A*) displayed an increase in T_{max} (Fig. 3*B*), the time to maximal LV elastance, indicative of prolonged ejection duration. TG-RLC(P−) also showed a decrease in maximal elastance (E_{max}) (Fig. 3*B*), consistent with our measurement of the end systolic pressure-volume relation (Fig. 2*B*). The prolonged time to end systole in TG-RLC(P−) suggested that these hearts were stiffer in that actin-myosin cross-bridges sustained pressure longer during systole; however TG-RLC(P−) hearts were overall more compliant, which was evidenced by a greater change in volume per unit pressure (decrease in E_{max}). Following dobutamine stimulation, absolute contractility indexed by E_{max} significantly increased in NTG animals and slightly decreased in TG-RLC(P−); however, ejection time was accelerated in TG-RLC(P−) to match that of NTG, which did not change with β-adrenergic stimulation, consistent with Ref. 30. These data demonstrate that RLC phosphorylation correlates with maximal ventricular elasticity, but not kinetics, during ejection.

TG-RLC(P−) Displayed a Significantly Blunted Response to Acute Dobutamine Infusion—Fig. 4 (*A* and *B*) illustrates pressure-volume loops from NTG and TG-RLC(P−) at base line and following dobutamine stress (5 ng/g of body weight/min)

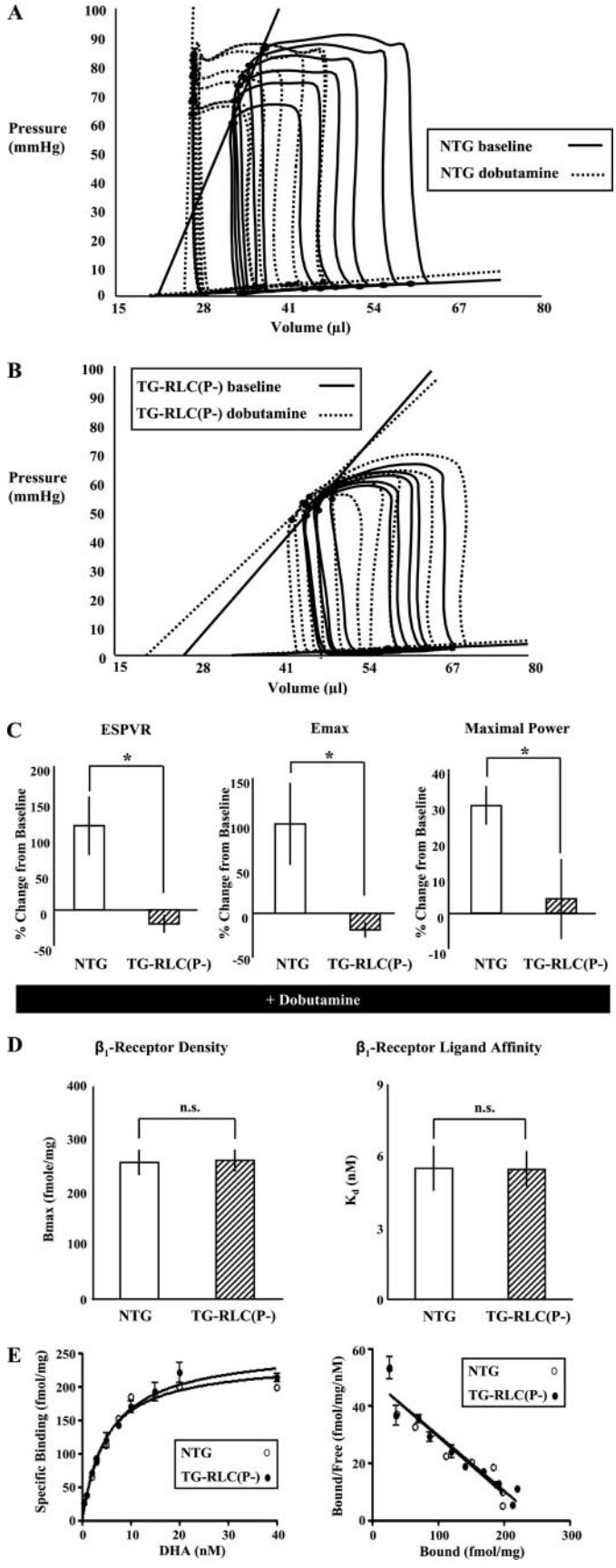

FIGURE 4. **TG-RLC(P−) show a blunted response to dobutamine that is not due to alterations in β_1 receptors.** *A* and *B*, representative pressure-volume loops from NTG (*A*) and TG-RLC(P−) (*B*) at base line (*solid lines*) and following dobutamine (5 ng/g of body weight/min (intravenously), *dashed lines*). *C*, percent changes in contractile parameters from base line are shown from paired experiments, $n = 8$–11. *D*, comparison of the density (B_{max}) and dissociation constant (K_d) of cardiac β_1-adrenergic receptors in LV membrane preparations. *E*, saturation binding of [^{3}H]dihydroalprenolol to cardiac sarcolemmal membranes and the Scatchard plots of data prepared from NTG and TG-RLC(P−) mice ($n = 3$). The *asterisk* denotes statistical significance ($p < 0.05$).

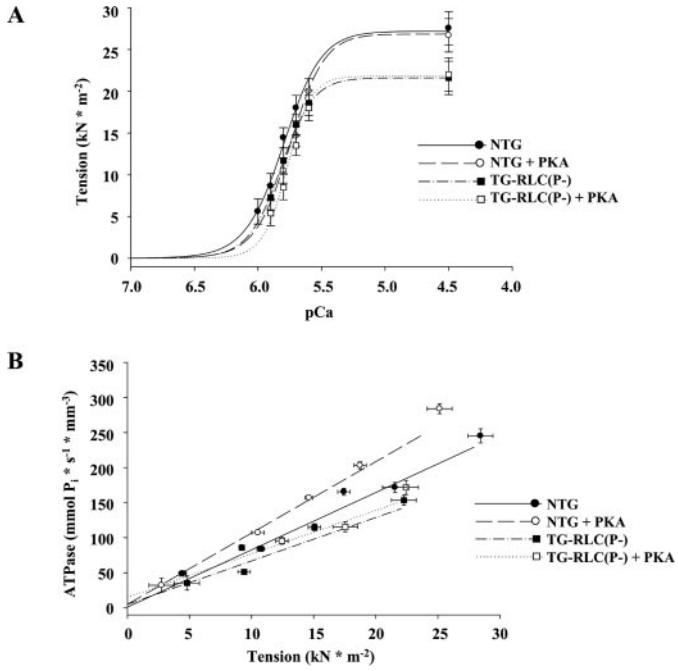

FIGURE 5. **TG-RLC(P−) mice have altered *in vitro* mechanical properties that are not normalized by PKA treatment.** *A*, Ca^{2+}-dependent tension relationships of trabeculae from NTG (*circles*) or TG-RLC(P−) (squares) with (*open symbols*) and without (*filled symbols*) PKA treatment (50 units, 1 h at 20 °C). Tension-calcium measurements fit to a modified Hill equation, determined decreased maximum Ca^{2+}-activated tension (pCa = 4.5) production in TG-RLC(P−), with similar Ca^{2+} sensitivity (pCa_{50}) to NTG. PKA treatment decreased Ca^{2+} sensitivity of both NTG and TG-RLC(P−). *B*, simultaneous assessment of tension production and energy expenditure determined decreased tension cost in TG-RLC(P−). PKA incubation significantly increased tension cost in NTG, whereas significance was not reached in TG-RLC(P−) preparations ($n = 5$–9).

for 5 min. NTG showed a significant left shift in their pressure-volume relation and an increase in the slope of their ESPVR (Fig. 4*C*). In contrast, TG-RLC(P−) demonstrated little change with respect to load-independent measures of contractility (ESPVR and E_{max}) and maximal power (Fig. 4*C*). This lack of response was not due to altered β-adrenergic receptor density or binding affinity, which we determined to be the same (B_{max} = 256.0 NTG *versus* 259.7 fmol/mg TG-RLC(P−), K_d = 5.46 NTG *versus* 5.43 nmol/L TG-RLC(P−); Fig. 4, *D* and *E*). These data indicate that RLC phosphorylation may be critical in eliciting a functionally normal β_1-adrenergic response.

Skinned Fiber Mechanics Were Altered in TG-RLC(P−), Both at Base Line and Following PKA Phosphorylation—Maximal Ca^{2+}-activated isometric tension in skinned fibers was lower in TG-RLC(P−) (27.1 ± 1.4 NTG, 21.6 ± 0.7 TG-RLC(P−) mN mm^{-2}) with no significant change in Ca^{2+} sensitivity (pCa_{50} (the negative log of the calcium concentration at half-maximal tension) = 5.80 ± 0.04 *versus* 5.82 ± 0.01, TG-RLC(P−) and NTG, respectively) (Fig. 5*A*). In addition, the economy of force

production, or tension cost (ATPase/force), was significantly decreased in TG-RLC(P−) (5.8 ± 0.5 pmol s^{-1} mm^{-1} mN^{-1}) trabeculae as compared with NTG (8.8 ± 1.0 pmol s^{-1} mm^{-1} mN^{-1}) (Fig. 5*B*). Following incubation with PKA, there was a desensitization to Ca^{2+} in both TG-RLC(P−) and NTG fibers, $\Delta pCa_{50} = 0.05$ and 0.05, respectively. Tension cost significantly increased in NTG fibers (10.7 ± 1.3 pmol s^{-1} mm^{-1} mN^{-1}) with PKA treatment; however, the increase in TG-RLC(P−) fibers (6.2 ± 0.4 pmol s^{-1} mm^{-1} mN^{-1}) tension cost did not reach significance.

TG-RLC(P−) Sarcomeres Had a Reduced Level of TnI and MyBP-C Phosphorylation at Base Line That Rose to the Same

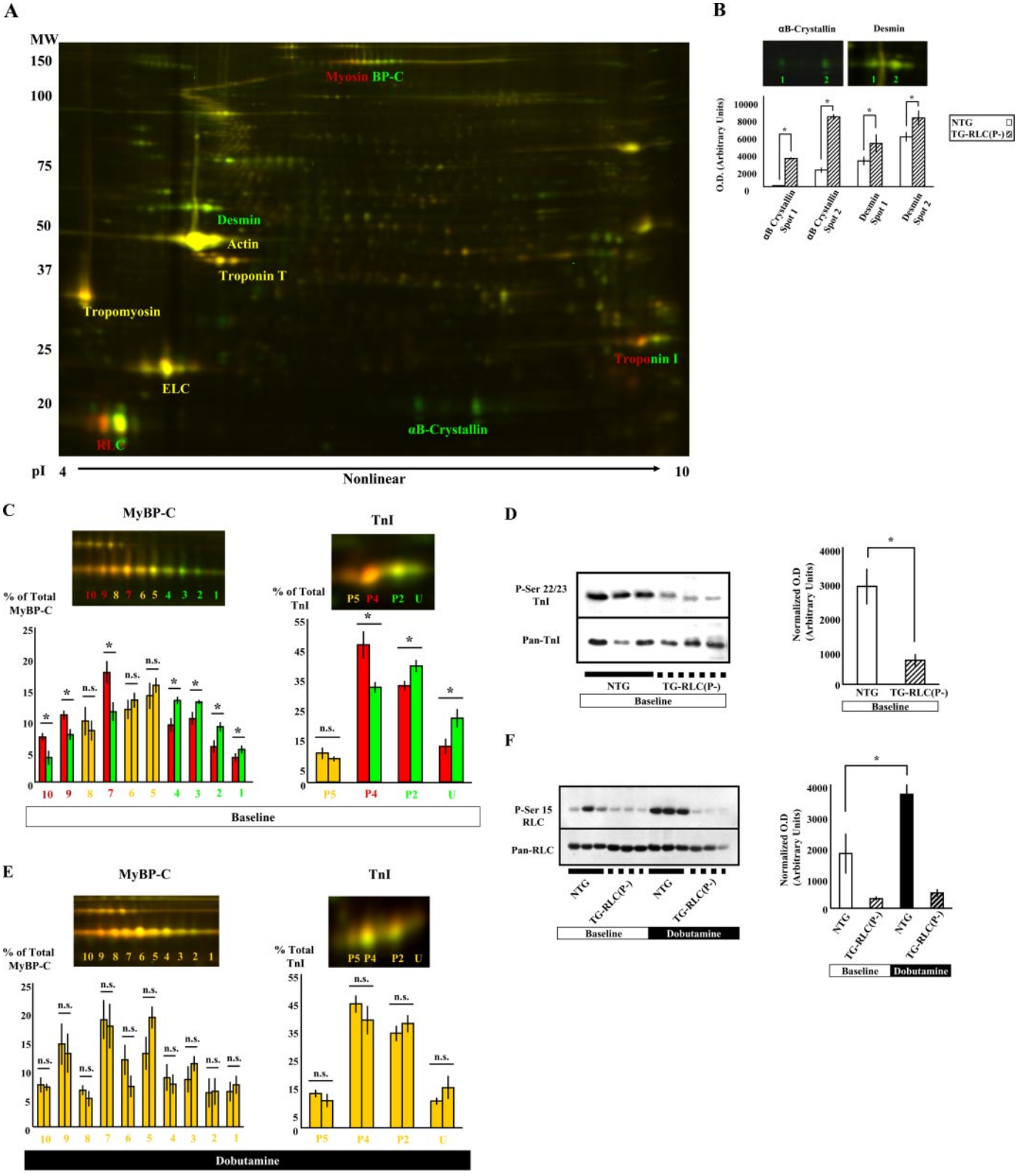

Levels as NTG Controls with Dobutamine Treatment; thus, the Only Sarcomeric Difference in Phosphorylation Following β_1-Adrenergic Stimulation Was at RLC Ser^{15}—We compared the global proteome of TG-RLC(P−) and NTG sarcomeres using two-dimensional difference gel electrophoresis. Homogenates from hearts of NTG and TG-RLC(P−) were labeled with fluorescent Cy dyes 5 and 3, respectively, and separated in the first dimension over a broad pI range (3–11) to examine all of the myofilament proteins simultaneously. Fig. 6*A* shows a representative two-dimensional map of the cardiac sarcomeric proteome. Labeled proteins were identified with mass spectrometry (data not shown) and were consistent with identifications made previously (24, 31). Increases in abundance of the Z-disk protein, desmin, and the small heat shock protein, α-B crystallin, were detected and are quantified in Fig. 6*B*. Both proteins have been shown to be up-regulated in cardiac pathology; however, the overexpression of neither desmin nor α-B crystalline have generated an observable phenotype (32, 33); therefore the significance of these results remains unknown. There were decreases in base-line phosphorylation of both TnI and MyBP-C in TG-RLC(P−) sarcomeres, which manifested as a gradient of color in the trail of spots (Fig. 6*C*). MyBP-C resolved as 10 distinct charged species, consistent with previous analysis (24), and TnI as four species consistent with previous analysis of mice at this age (34). Although we could not unequivocally identify all 10 MyBP-C spots, we concluded that there was a relative depression in MyBP-C phosphorylation based upon the presence of more abundant NTG spots in the acidic pole and the more abundant TG-RLC(P−) spots in the basic pole of the spot trail. We have previously identified unphosphorylated (U) and phosphorylated (P2, P4, and P5) spots in TnI (34). In agreement with our previous observations (34), TnI was highly phosphorylated at base line (88%) in NTG and was significantly less (78%) in TG-RLC(P−). To determine the specific site(s) of TnI de phosphorylation in TG-RLC(P−), we probed myofibrillar proteins with a phospho-specific serine 22/23-TnI antibody and observed that TnI was dephosphorylated specifically at serines 22/23 (Fig. 6*D*). Importantly, dobutamine administration abolished these differences indicating the competency of MyBP-C and TnI as PKA substrates downstream of β_1-adrenergic stimulation in TG-RLC(P−) (Fig. 6*E*). To determine whether RLC was a specific target of phosphorylation involved in the attenuated functional response to dobutamine, we probed RLC with a Ser(P)^{15}-specific antibody. In NTG animals, RLC showed a striking increase in phosphorylation following acute dobutamine stimulation, an effect significantly blunted in RLC(P−) animals by the substitution of alanine at this site (Fig. 6*F*). These data indicate that the lack of phosphorylation potential in TG-RLC(P−) RLC contributes to the blunted positive inotropic response of TG-RLC(P−) to β_1-adrenergic stimulation.

DISCUSSION

Our studies provide new insights into the significant role of RLC phosphorylation in systolic mechanics in basal conditions and in response to adrenergic stimulation. Although in basal conditions the lack of RLC phosphorylation was associated with relatively depressed phosphorylation of cTnI at serines 22/23 and MyBP-C, the lack of functional response to dobutamine was not associated with differences in cTnI and MyBP-C phosphorylation from controls. The functional deficit may have been causally linked with the inability of TG-RLC(P−) to increase phosphorylation of RLC at alanine-substituted serine-15 following acute dobutamine stimulation, because there was a parallel and robust increase in NTG controls. A major conclusion from our studies is that phosphorylation of RLC is important to normal cardiac function.

Our hypothesis for the mechanism of the deficit in function associated with lack of RLC phosphorylation is couched in terms of our current understanding of the structural and functional effects of RLC phosphorylation and current theories of sarcomere-related mechanisms of ejection. RLC phosphorylation has been reported to induce a radial movement of myosin heads away from the thick filament. This radial movement of the myosin heads increases the local concentration of cross-bridges at its interface with thin filaments and is presumably responsible for an increase in the ratio of strong to weak force-generating attachments (35, 36). In view of our findings with regard to loss of systolic power and prolongation of ejection in the absence of RLC phosphorylation, we think these changes in the structure of RLC and cross-bridge actions indicate that regulation of ejection involves an essential role of mechanisms at the level of the sarcomere. In support of this idea, MyBP-C phosphorylation, which induces a strikingly similar structural change as RLC phosphorylation (37), has been demonstrated to be essential to normal systolic mechanics (30, 38). Moreover, except for a mouse model with ablation of MyBP-C (39) and the TG-RLC(P−) studied here, time from onset of ejection to time to end systole has been shown to be resistant to other sarcomeric protein modifications. Of particular interest were the simultaneous acceleration of ejection time and decrease in absolute contractility in TG-RLC(P−) following β_1-adrenergic

FIGURE 6. **Two-dimensional difference gel electrophoresis of the global myofilament proteome and Western blotting analysis reveal significant changes in protein phosphorylation between TG-RLC(P−) and NTG mice.** *A*, TG-RLC(P−) and NTG proteins were labeled with Cy3 and Cy5, respectively. The proteins were focused in the first dimension using a broad 3-11, nonlinear isoelectric point range, and by 12% SDS-PAGE in the second dimension. The proteins in *yellow text* were not different in abundance between TG-RLC(P−) and NTG, proteins in *green text* were more abundant in TG-RLC(P−), and proteins in *two-color text* showed a difference in phosphorylation. Two-dimensional spots were quantified using PDQuest (Bio-Rad). Two-dimensional maps were normalized against total spot density to eliminate differences in system gain. *B*, desmin and α-B crystallin abundance were both significantly increased in TG-RLC(P−) at base line as indicated by the green color of these protein spots. *C*, MyBP-C and TnI were dephosphorylated at base line in TG-RLC(P−) (*green*) relative to NTG (*red*). *D*, one-dimensional SDS-PAGE (12%) and Western blotting using anti-Ser(P)$^{22/23}$ TnI antibody revealed that the specific sites at which TnI is dephosphorylated in TG-RLC(P−) are in the N-terminal cardiac-specific region of TnI. Ser(P)$^{22/23}$ densities were normalized against pan-TnI densities and normalized densities are shown in the bar graph. *E*, following acute dobutamine stimulation, phosphorylation differences were abolished in both MyBP-C and TnI; however, in comparing RLC phosphorylation in base line- and dobutamine-treated NTG and TG-RLC(P−) (*F*), it became apparent that although TG-RLC(P−) were prevented from increasing ser15-RLC phosphorylation following dobutamine treatment (*hatched bars*), NTG animals demonstrated a robust increase (solid bars), which may explain the dramatically blunted functional effect observed in TG-RLC(P−) following β_1-stimulation. The *asterisk* denotes statistical significance ($p < 0.05$; $n = 5$–7).

stimulation. Although increased MyBP-C phosphorylation in the cardiac-specific domain cannot for these observations (30), TnI phosphorylation may be a likely candidate for regulating ejection timing, whereas RLC phosphorylation may be more critical for modulating maximal elastance. However, both RLC (40) and MyBP-C phosphorylation (41) enhance stretch activation, a mechanical property inherent to the sarcomere and thought to sustain power during cardiac ejection (42). Computational models, which support this important role of sarcomere-based mechanisms in ejection and isovolumic relaxation, indicate that the time course of Ca^{2+} bound to TnC is nearly over at a time when ejection is ongoing and isovolumic relaxation has not yet begun (15). RLC is a likely candidate for a central role in these mechanisms based upon its position at the fulcrum of the lever arm (S1-S2 junction of myosin heavy chain) (16), its ability to be modulated by charge (43), and its close proximity to another thick filament protein important in modulating cardiac mechanics, MyBP-C (44).

Our finding of a critical role of RLC phosphorylation in hearts stimulated with dobutamine, which supports previous studies of load-dependent parameters by Sanbe *et al.* (10), also provides evidence of its vital role in regulation of cardiac contractility. Our studies provide a novel biochemical mechanism for the blunted response of TG-RLC(P−) hearts to dobutamine by the demonstration of a substrate phosphorylation at RLC serine 15 in NTG controls following dobutamine that could not occur in TG-RLC(P−) hearts. Previous studies examined whether β-adrenergic stimulation altered RLC phosphorylation in isolated, isovolumic Langendorff heart preparations (4, 43, 45–47), and most found little to no change. One major difference between these studies and the current study was that we used an *in vivo* model to scrutinize the systolic ejection phase. Furthermore, most of the aforementioned studies involved perfusion of hearts with a β-agonist for short periods of time (20–40 s) to capture RLC phosphorylation levels that paralleled peak LV pressure. Interestingly, Westwood and Perry (47) compared RLC phosphorylation at 30 s (peak response) and 5 min (post-peak response) and reported an increase in RLC phosphorylation only when hearts were harvested at a time post-peak response. Consequently, we measured RLC phosphorylation at a later (5 min post-onset of dobutamine) time point at which LV pressure and first derivative of the maximal rate of change in pressure divided by time (dp/dt) were elevated but not maximal. We demonstrated that at this time point RLC phosphorylation was increased at serine 15 and therefore appeared to play a role in β_1-adrenergic signaling along with neighboring sarcomeric proteins TnI and MyBP-C. To our knowledge, this is the first report demonstrating an increase in RLC serine 15 phosphorylation *in vivo* in response to dobutamine treatment. Importantly, in TG-RLC(P−) animals that could not be phosphorylated at serine 15, RLC was the only sarcomeric protein demonstrating a difference in phosphorylation following dobutamine treatment (Fig. 6*F*) and thus stands as the sole sarcomeric link to the dysfunction observed.

The recent demonstration of a novel cardiac-specific MLCK present at 10–20-fold greater than smooth muscle MLCK in heart (48) offered further insight into our findings. Chan *et al.* (48) reported that in response to phenylephrine treatment, both cardiac MLCK and RLC were phosphorylated independent of Ca^{2+} and calmodulin. This lack of control by Ca^{2+} and calmodulin may explain the lack of increase in phosphorylation of RLC observed in previous studies, which employed high perfusate Ca^{2+} as a means of increasing RLC phosphorylation (45, 46). Additionally, cardiac-specific MLCK has a unique N-terminal region housing multiple PKA consensus sites (our *in silico* analysis), thereby providing a plausible link between β-adrenergic receptor signaling, PKA activation, and downstream RLC phosphorylation.

Our studies with skinned fibers also generated the novel finding of a decreased economy of tension in TG-RLC(P−) fibers, suggesting a critical role for RLC phosphorylation in modulation of cardiac kinetics. In accordance with a simple two-state model of muscle contraction (49), where non-force- and force-generating states are determined by the rate constants of cross-bridge attachment and detachment, *f* and *g*, respectively, a decrease in tension cost suggests a decreased cycling kinetics in TG-RLC(P−) because of a decrease in *g*. This decrease in *g* supports our *in vivo* hemodynamic finding of sustained ejection time (increase in T_{max}). Therefore, TG-RLC(P−) cross-bridges may have a prolonged duty cycle, which manifests as slower and less powerful ejection kinetics during systole. Additionally, TnI phosphorylation at PKA sites (serine 22/23) has been shown to increase tension cost (50), and therefore the observed decrease in these sites at base line would assist in explaining the parallel decrease in tension cost, irrespective of changes in RLC phosphorylation. Interestingly, although exogenous PKA treatment increased tension cost in NTG animals as previously reported (50), normalization to NTG values did not occur in TG-RLC(P−), although achieving normal levels of TnI phosphorylation. This further suggests that phosphorylation levels of RLC may play a coordinate role in modulating tension cost with TnI. Our other measures of skinned fiber function generally agreed with earlier data from studies employing *in vitro* MLCK phosphorylation, which induced increases in tension (8, 11, 40), and ATPase (10, 51). However, in contrast to reports of an increase in Ca^{2+} sensitivity with RLC phosphorylation (8, 51), we found no difference between TG-RLC(P−) and NTG, most likely because of decreased TnI phosphorylation in the TG-RLC(P−) fibers. Previous studies have also observed parallel changes in TnI and RLC phosphorylation. For example, Pi *et al.* (52) reported transgenic mice expressing nonphosphorylatable PKC sites on TnI (S43A/S45A/S144A) possessed a modest decrease in RLC phosphorylation, and these fibers could not be further sensitized to Ca^{2+} by MLCK treatment. Our data also showed an increase in TnI phosphorylation with PKA desensitizes TG-RLC(P−) fiber tension to Ca^{2+}. In contrast to TnI, our study is the first, to our knowledge, to report parallel changes in RLC and MyBP-C phosphorylation.

Previous studies have supported the notion that the net negatively charged phosphorylation of the RLC N terminus repels the negatively charged myofilament backbone and positions myosin heads away from the thick filament backbone, bringing them in closer proximity to actin, thereby promoting the actin-cross-bridge interaction (17). Thus, one might predict that in TG-RLC(P−) animals, as the phosphorylatable RLC becomes replaced with one rendered nonphosphorylatable, the resulting

net positive charge on RLC may promote a stronger interaction with the negatively charged filament backbone, effectively increasing the distance between myosin heads and actin. The crystal structure of chicken skeletal myosin subfragment 1, resolved by Rayment *et al.* (16), localized the phosphorylatable N-terminal region of RLC near the fulcrum of the lever arm. Interestingly, it has been demonstrated that the cardiac-specific, phosphorylatable region of MyBP-C binds S2 near this hinge region of myosin (53). MyBP-C has been described as a brake on myosin by creating an internal load on the cardiac sarcomere (54). In studies where MyBP-C has been ablated, isolated cardiac cells demonstrated increases in cross-bridge cycling rate, shortening velocity, and power output (55). Importantly, and of particular relevance to our findings of altered MyBP-C phosphorylation in TG-RLC(P−), the interaction of MyBP-C and the S2 hinge were abolished by PKA-mediated phosphorylation, thus effectively releasing the brake on myosin (53). It remains to be experimentally determined whether phosphorylatable N-terminal regions of RLC and MyBP-C interact and jointly modulate the position of myosin heads with respect to actin and the thick filament backbone, because it is highly likely that these regions are not mutually exclusive.

The importance of RLC phosphorylation, particularly with respect to heart failure, has been underscored in studies demonstrating decreased levels of RLC phosphorylation associated with a decline in function in failing human hearts (56–58). Interestingly, the function of the TG-RLC(P−) mice used in our study resembles that of a heart failure patient both at the ventricular chamber and biochemical levels. Similarities at the organ level include depressed i*n vivo* function as indexed by decreased contractility, ejection fraction, and LV pressure. An interesting difference, however, is the lack of concomitant dilatation in TG-RLC(P−) hearts. Furthermore, as in heart failure, TG-RLC(P−) hearts were insensitive to β-adrenergic stimulation; however, we could not attribute the lack of response in TG-RLC(P−) to a decreased β-receptor density as is observed clinically. At the biochemical level, TnI phosphorylation was decreased, which has been shown in human heart failure (57, 59), and MyBP-C phosphorylation was decreased as has been shown in animal models of heart failure (38). The striking similarities of the TG-RLC(P−) model with human heart failure highlight the critical role of RLC phosphorylation in maintaining normal cardiac function.

Acknowledgments—We thank Chad M. Warren for assistance in the analysis of myosin heavy chain isoforms. We also thank Dr. Neal Epstein at the National Institutes of Health for the generous gift of phospho-RLC antibody.

REFERENCES

1. Solaro, R. J., and Rarick, H. M. (1998) *Circ. Res.* **83,** 471–480
2. Solaro, R. J. (2001) in *Handbook of Physiology: The Cardiovascular System*, Vol. 1: The Heart, pp. 264–300, Oxford University Press, Oxford
3. Frearson, N., and Perry, S. V. (1975) *Biochem. J.* **151,** 99–107
4. Holroyde, M. J., Small, D. A., Howe, E., and Solaro, R. J. (1979) *Biochim. Biophys. Acta* **587,** 628–637
5. Barany, K., Sayers, S. T., DiSalvo, J., and Barany, M. (1983) *Electrophoresis.* **4,** 138–142
6. Poetter, K., Jiang, H., Hassanzadeh, S., Master, S. R., Chang, A., Dalakas, M. C., Rayment, I., Sellers, J. R., Fananapazir, L., and Epstein, N. D. (1996) *Nat. Genet.* **13,** 63–69
7. Morano, I., Arndt, H., Bachle-Stolz, C., and Ruegg, J. C. (1986) *Basic Res. Cardiol.* **81,** 611–619
8. Sweeney, H. L., and Stull, J. T. (1986) *Am. J. Physiol.* **250,** C657–C660
9. Morano, I., Bachle-Stolz, C., Katus, A., and Ruegg, J. C. (1988) *Basic Res. Cardiol.* **83,** 350–359
10. Sanbe, A., Fewell, J. G., Gulick, J., Osinska, H., Lorenz, J., Hall, D. G., Murray, L. A., Kimball, T. R., Witt, S. A., and Robbins, J. (1999) *J. Biol. Chem.* **274,** 21085–21094
11. Olsson, M. C., Patel, J. R., Fitzsimons, D. P., Walker, J. W., and Moss, R. L. (2004) *Am. J. Physiol.* **287,** H2712–H2718
12. Davis, J. S., Hassanzadeh, S., Winitsky, S., Lin, H., Satorius, C., Vemuri, R., Aletras, A. H., Wen, H., and Epstein, N. D. (2001) *Cell* **107,** 631–641
13. Davis, J. S., Satorius, C. L., and Epstein, N. D. (2002) *Biophys. J.* **83,** 359–370
14. Davis, J. S., Hassanzadeh, S., Winitsky, S., Wen, H., Aletras, A., and Epstein, N. D. (2002) *Cold Spring Harb. Symp. Quant. Biol.* **67,** 345–352
15. Hinken, A. C., and Solaro, R. J. (2007) *Physiol.* (*Bethesda*) **22,** 73–80
16. Rayment, I., Rypniewski, W. R., Schmidt-Base, K., Smith, R., Tomchick, D. R., Benning, M. M., Winkelmann, D. A., Wesenberg, G., and Holden, H. M. (1993) *Science* **261,** 50–58
17. Sweeney, H. L., Bowman, B. F., and Stull, J. T. (1993) *Am. J. Physiol.* **264,** C1085–C1095
18. Solaro, R. J., Pang, D. C., and Briggs, F. N. (1971) *Biochim. Biophys. Acta* **245,** 259–262
19. Montgomery, D. E., Rundell, V. L., Goldspink, P. H., Urboniene, D., Geenen, D. L., de Tombe, P. P., and Buttrick, P. M. (2005) *Am. J. Physiol.* **289,** H1881–H1888
20. Suga, H., and Sagawa, K. (1974) *Circ. Res.* **35,** 117–126
21. Fritz, J. D., Swartz, D. R., and Greaser, M. L. (1989) *Anal. Biochem.* **180,** 205–210
22. Baker, S. P., and Potter, L. T. (1980) *Membr. Biochem.* **3,** 185–205
23. Thawornkaiwong, A., Preawnim, S., and Wattanapermpool, J. (2003) *Life Sci.* **72,** 1813–1824
24. Yuan, C., Guo, Y., Ravi, R., Przyklenk, K., Shilkofski, N., Diez, R., Cole, R. N., and Murphy, A. M. (2006) *Proteomics* **6,** 4176–4186
25. Laemmli, U. K. (1970) *Nature* **227,** 680–685
26. Matsudaira, P. (1987) *J. Biol. Chem.* **262,** 10035–10038
27. Hinken, A. C., and McDonald, K. S. (2004) *Am. J. Physiol.* **287,** C500–C507
28. de Tombe, P. P., and Stienen, G. J. (1995) *Circ. Res.* **76,** 734–741
29. Suga, H., Sagawa, K., and Shoukas, A. A. (1973) *Circ. Res.* **32,** 314–322
30. Nagayama, T., Takimoto, E., Sadayappan, S., Mudd, J. O., Seidman, J. G., Robbins, J., and Kass, D. A. (2007) *Circulation* **116,** 2399–2408
31. Chu, G., Egnaczyk, G. F., Zhao, W., Jo, S. H., Fan, G. C., Maggio, J. E., Xiao, R. P., and Kranias, E. G. (2004) *Circ. Res.* **94,** 184–193
32. Wang, X., Osinska, H., Klevitsky, R., Gerdes, A. M., Nieman, M., Lorenz, J., Hewett, T., and Robbins, J. (2001) *Circ. Res.* **89,** 84–91
33. Wang, X., Osinska, H., Dorn, G. W., II, Nieman, M., Lorenz, J. N., Gerdes, A. M., Witt, S., Kimball, T., Gulick, J., and Robbins, J. (2001) *Circulation* **103,** 2402–2407
34. Scruggs, S. B., Walker, L. A., Lyu, T., Geenen, D. L., Solaro, R. J., Buttrick, P. M., and Goldspink, P. H. (2006) *J. Mol. Cell Cardiol.* **40,** 465–473
35. Metzger, J. M., Greaser, M. L., and Moss, R. L. (1989) *J. Gen. Physiol.* **93,** 855–883
36. Solaro, R. J. (2001) *Heart Physiology and Pathophysiology*, 4th Ed., pp. 519–526, Academic Press, Orlando, FL
37. Weisberg, A., and Winegrad, S. (1996) *Proc. Natl. Acad. Sci. U. S. A.* **93,** 8999–9003
38. Sadayappan, S., Gulick, J., Osinska, H., Martin, L. A., Hahn, H. S., Dorn, G. W., II, Klevitsky, R., Seidman, C. E., Seidman, J. G., and Robbins, J. (2005) *Circ. Res.* **97,** 1156–1163
39. Palmer, B. M., Georgakopoulos, D., Janssen, P. M., Wang, Y., Alpert, N. R., Belardi, D. F., Harris, S. P., Moss, R. L., Burgon, P. G., Seidman, C. E., Seidman, J. G., Maughan, D. W., and Kass, D. A. (2004) *Circ. Res.* **94,** 1249–1255
40. Stelzer, J. E., Patel, J. R., and Moss, R. L. (2006) *J. Gen. Physiol.* **128,** 261–272

41. Stelzer, J. E., Patel, J. R., Walker, J. W., and Moss, R. L. (2007) *Circ. Res.* **101,** 503–511
42. Epstein, N. D., and Davis, J. S. (2006) *Circ. Res.* **98,** 1110–1112
43. Frearson, N., Solaro, R. J., and Perry, S. V. (1976) *Nature* **264,** 801–802
44. Kunst, G., Kress, K. R., Gruen, M., Uttenweiler, D., Gautel, M., and Fink, R. H. (2000) *Circ. Res.* **86,** 51–58
45. Jeacocke, S. A., and England, P. J. (1980) *Biochem. J.* **188,** 763–768
46. High, C. W., and Stull, J. T. (1980) *Am. J. Physiol.* **239,** H756–H764
47. Westwood, S. A., and Perry, S. V. (1981) *Biochem. J.* **197,** 185–193
48. Chan, J. Y., Takeda, M., Briggs, L. E., Graham, M. L., Lu, J. T., Horikoshi, N., Weinberg, E. O., Aoki, H., Sato, N., Chien, K. R., and Kasahara, H. (2008) *Circ. Res.* **102,** 571–580
49. Huxley, A. F. (1957) *Prog. Biophys. Biophys. Chem.* **7,** 255–318
50. Biesiadecki, B. J., Kobayashi, T., Walker, J. S., John Solaro, R., and de Tombe, P. P. (2007) *Circ. Res.* **100,** 1486–1493
51. Clement, O., Puceat, M., Walsh, M. P., and Vassort, G. (1992) *Biochem. J.* **285,** 311–317
52. Pi, Y., Zhang, D., Kemnitz, K. R., Wang, H., and Walker, J. W. (2003) *J. Physiol.* **552,** 845–857
53. Gruen, M., Prinz, H., and Gautel, M. (1999) *FEBS Lett.* **453,** 254–259
54. Hofmann, P. A., Greaser, M. L., and Moss, R. L. (1991) *J. Physiol.* **439,** 701–715
55. Korte, F. S., McDonald, K. S., Harris, S. P., and Moss, R. L. (2003) *Circ. Res.* **93,** 752–758
56. van der Velden, J., Papp, Z., Boontje, N. M., Zaremba, R., de Jong, J. W., Janssen, P. M., Hasenfuss, G., and Stienen, G. J. (2003) *Cardiovasc. Res.* **57,** 505–514
57. van der Velden, J., Papp, Z., Zaremba, R., Boontje, N. M., de Jong, J. W., Owen, V. J., Burton, P. B. J., Goldmann, P., Jaquet, K., and Stienen, G. J. M. (2003) *Cardiovasc. Res.* **57,** 37–47
58. van Der Velden, J., Klein, L. J., Zaremba, R., Boontje, N. M., Huybregts, M. A., Stooker, W., Eijsman, L., de Jong, J. W., Visser, C. A., Visser, F. C., and Stienen, G. J. (2001) *Circulation* **104,** 1140–1146
59. Morano, I., Hadicke, K., Haase, H., Bohm, M., Erdmann, E., and Schaub, M. C. (1997) *J. Mol. Cell Cardiol.* **29,** 1177–1187